Nanofiltration membranes with dually charged composite layer exhibiting super-high multivalent-salt rejection

Chunrui Wu[a, *], Sihua Liu[a], Zhongyang Wang[a], Jianhua Zhang[b], Xuan Wang[a], Xiaolong Lu[a, *], Yue Jia[a], Weisong Hung[c], Kuiran Lee[c]

[a] *State Key Laboratory of Separation Membranes and Membrane Processes, Institute of Biological and Chemical Engineering, Tianjin Polytechnic University, Tianjin, 300387, P.R. China*

[b] *Institute of Sustainability and Innovation, Victoria University, PO Box 14428, Melbourne, Victoria 8001, Australia*

[c] *R&D Center for Membrane Technology and Department of Chemical Engineering, Chung Yuan University, 200 Chung-pei Rd., Chung-Li, Taoyuan 32023, Taiwan, China*

*Corresponding authors. Tel. /fax: +86 22 83955170.

E-mail addresses: wuchunrui@tjpu.edu.cn (C. Wu), luxiaolong@263.net (X. Lu).

Abstract

State-of-the-art nanofiltration (NF) membranes generally positively or negatively charged could not remove both multivalent cations and anions once and for all according to the Donnan Exclusion. Designing NF membranes with facile approach for effective removal of multivalent-salt without compromising the permeation is still a tough challenge. In this work, we demonstrate a sort of novel NF membrane consists of a positively charged interlayer sandwiched between substrate and negatively charged outermost surface. The restructured NF membranes with dually charged composite layer were fabricated via amination-interfacial polymerization (A-IP) on poly (vinyl chloride) (PVC) substrate. The resultant NF membranes exhibited super high salts rejection of up

to 99.0% $MgCl_2$, 99.0% $MgSO_4$, 98.5% $CaCl_2$, 95.7% $Pb(NO_3)_2$, and 96.0% Na_2SO_4. Additionally, reasonably high flux (8.7 $L \cdot m^{-2} \cdot h^{-1} \cdot bar^{-1}$, (pure water permeability (PWP))) approaching those of commercial NF membranes was obtained due to the relatively loose structure of the composite layer. Furthermore, the transport and separation mechanism of the restructured NF membranes reveals that the significant upgraded separation performance could be attributed to the synergistic effect of the dually charged layer.

Keywords: Nanofiltration membrane; Dual charged composite layer; Amination; Interfacial polymerization; Donnan exclusion

1. Introduction

Water scarcity is attracting concerning worldwide, due to increasing requirement i.e., population growth and industrialization, and reduction of available freshwater resources caused by pollution and climate change [1-2]. To protect and broaden the freshwater resources, various efforts have been made for environmentally friendly wastewater discharge and recycling [3-4]. Membrane separation technique has become one of the essential technologies in most of the wastewater reuse plant, because of its advantages such as small footprint, flexible design, low chemical consumption and highly automated operation [5-6].

Hardness and heavy metal removals are the key issues in drinking water treatment. As the intermediate membrane technology between ultrafiltration and reverse osmosis, nanofiltration (NF) has become one of the most promising technologies for water softening and the removal of heavy metal ions [7-10]. State-of-the-art commercial NF membranes usually possess a composite structure consisting of a porous support and an ultra-thin active layer generally positively or negatively charged [11-14]. Most of the commercial NF membranes synthesized via interfacial polymerization (IP) are negatively charged during normal aqueous processes. According to the Donnan exclusion, the negatively charged NF membranes tend to exhibit excellent rejection to multivalent anions (e.g., $Cr_2O_7^{2-}$, SO_4^{2-}) and relatively low rejection to multivalent cations (e.g., Mg^{2+}, Ca^{2+}) [15-16]. For example, Hilal et al. studied the rejection of heavy metal ions using NF270 membrane and the results showed that with all metals examined (except As (III)), when the feed pH is below the isoelectric point at pH around 4, the rejection increased. However, at pH above 4 the average rejections decreased [8]. Meanwhile, NF270 membranes failed in water softening processes with only about 60 % hardness removal [17]. In contrast, NF membranes with positive surface charges would be ideal for water softening and heavy metal removal intuitively. Nevertheless, positively charged NF membranes exhibited relatively low rejection towards multivalent anions (e.g., $Cr_2O_7^{2-}$, SO_4^{2-}, $AsHO_4^{2-}$) [18-19]. Moreover, during filtration

processes, counter-ions and suspended colloids can be easily absorbed on the positively charged surface to partially weaken the electrostatic repulsion and accelerate membrane fouling [20-21]. Hence, an economic and efficient technology towards tailoring composite membranes exhibiting both excellent rejection to multivalent cations and anions is highly desired.

To achieve that target, many research works have been done. D. H. Wu et.al, applied two cycles of interfacial polymerization on a microporous polyether sulfone (PES) membrane, which showed outstanding retention towards $MgCl_2$ (rejection ≈ 98 %). However, the membrane exhibited a relatively low rejection (rejection ≈ 68 %) to Na_2SO_4 subjected to the Donnan Exclusion effect [22]. C. Ba and J. Economy reported a neutrally charged NF membrane fabricated by coating a layer of sulfonated poly (ether ether ketone) on a positively charged NF membrane [23]. To nicely remove heavy metals from wastewater, Z. W. Thong and co-workers developed a novel NF membrane consisting of a sulfonated pentablock copolymer rejection layer on a polyethylenimine-modified substrate [18]. These two types of reported membranes could remove multivalent ions (both cations and anions) efficiently. Nevertheless, they display a relatively low flux of 3 and 2.4 $L \cdot m^{-2} \cdot h^{-1} \cdot bar^{-1}$, respectively, attributing to the diminished effective pore diameter.

It is well recognized that the separation of the ionic species using NF membrane is

mainly based on both size exclusion and electrostatic interaction. As specified previously, the rejection of NF membrane could be improved by methods of decreasing pore diameter, while the flux would be lowered simultaneously. By improving the charge capacity of the membrane surface, more positively or negatively charged, could only improve the rejection to multivalent cations or anions, respectively [24-25]. Therefore, using facile approach to develop NF membranes with dually charged composite layers is of great significance. However, to the best of our knowledge, it is hardly to find study about preparation of NF membranes with dually charged composite layers.

Poly (vinyl chloride) (PVC) has attracted much interest because of its excellent mechanical strength, low cost, low toxicity and excellent chemical resistance properties. PVC membranes have been widely applied in water treatment and exhibited ideal separation properties [26-27]. More interestingly, substantial research about PVC modification has illustrated the presence of labile chlorine atoms and nucleophilic substitution has been the most studied reaction by far [28]. Among which, Amino-PVC produced by amination of PVC with polyamine always serve as a linkage for further functionalization [29-31]. Composite membranes using PVC as support material will be prone to optimization via appropriate reaction, and lower cost than that of the typical support materials (e.g., PSF, PES, PAN, et al.). However, there is hardly to find any

literature reporting preparation of NF membranes on PVC substrate.

In this work, we report a novel composite membrane consists of a positively charged interlayer sandwiched between substrate and negatively charged outermost surface. A facile method for preparing the dually charged composite layer NF membranes via amination-interfacial polymerization (A-IP) on PVC substrate was presented. The introduced positively charged interlayer was supposed to strengthen electrostatic interaction and then enhance salts rejection. The amination reaction was verified by fourier transform infrared spectroscopy (FT-IR) and x-ray photoelectron spectrometer (XPS) measurements. Zeta potential was used to investigate the charged properties of the interlayer and outermost surface of the prepared NF membranes. Doppler broadening energy spectroscopy (DBES), conducted using position annihilation spectroscopy (PAS) coupled with a variable mono-energy slow positron beam, was used to examine the membrane micro-structure as a function of positron incident energy. Transport and separation mechanism of the restructured NF membranes was also explored.

2. Materials and methods

2.1. Materials

PVC and PES hollow fiber ultrafiltration membranes with molecular weight cut-off

of 100 k Da were provided by Shenzhen Chengdelai Industry Co. Ltd. (China). Membrane modules were prepared for NF membranes preparation by potting a bunch of hollow fibers (5 fibers) into a nylon tube with an inside diameter of 6mm. Sodium chloride (NaCl), calcium chloride ($CaCl_2$), magnesium chloride ($MgCl_2$), magnesium sulfate ($MgSO_4$), sodium sulfate (Na_2SO_4), glucose, sucrose (Tianjin Guangfu Technology Development Co. Ltd. (China)) and lead nitrate ($Pb(NO_3)_2$, Tianjin Fengchuan Chemical Reagent Science And Technology Co. Ltd. (China)) were used for NF performance tests. N, N-dimethylacetamide (DMAc, >99%) purchased from Samsung Company (South Korea) was used to peel off the PVC support membrane. PIP (purity ≥ 99%) purchased from Tianjin Kemiou Chemical Reagent Co. Ltd. (China) and TMC (purity ≥ 99%) obtained from J&K Scientific Co. Ltd (China) were used as active monomers in aqueous phase and organic phase, respectively. In the preparation of PIP solution and TMC solution, deionized water and n-hexane (Tianjin Yingda Rare Chemical Reagents Factory (China)) were used, respectively. All the reagents were used as received.

2.2. Membrane fabrication

NF membranes: The schematic of the restructured membrane fabrication process was shown in Fig. 1, where PIP amination process was carried out before polymerization

with TMC. Different from common coating process, there are two kinds of PIP molecules: the adsorbed ones and the grafted ones after amination of PVC membranes. The amination of PVC hollow fiber membranes was carried out by immersing membrane modules into the PIP aqueous solutions at 70 ℃ for 120 min. After PIP amination, the excess PIP solution on the lumen side was removed by air sweeping at a flow rate of 8 m/s for 5 min. The IP was then directly incurred by circulating 0.10 % TMC/hexane solution through the lumen side of the membranes for 2 min. Finally, the synthetized membranes (ANFx membrane, x represent PIP concentration of (w/v)) were dried at ambient temperature for 15 min and then washed by and kept in deionized water before characterization. For comparison purpose, membranes (NF-PES membranes) using PES membrane instead of PVC membrane as substrate were fabricated with the same technic. Membranes (NF-PVC membranes) via conventional IP technic on PVC substrate were also fabricated. Both NF-PES and NF-PVC membranes were prepared under a PIP concentration of 1.0 % (w/v).

APVC membranes: To verify the amination reaction, APVC membranes were also fabricated through amination by PIP at 70 ℃ for 120 min and rinsed thoroughly. The rinsing process was performed by rinsing the aminated membranes with deionized water until the pH value was kept steady at 6.5. Subsequently, an ultrafiltration process was conducted at 0.15 MPa for 30min to remove the PIP molecules absorbed in pore

channels. The rinsed PVC fibers were soaked into deionized water for 3 days and the deionized water was changed daily before characterization.

2.3. Membrane characterization

FT-IR spectra were collected using a Vector-22 spectrometer (Bruker Daltonic Inc., Germany) with Zinc Selenide (ZnSe) as an internal reflection element at an incident angle of 45º. Each spectrum was collected by the accumulation of 16 scans at a resolution of 4 cm^{-1}. XPS measurements were performed on a Quanta 200 spectrometer (FEI Co., Ltd. USA) using monochromatized AlKa radiation at 1486.6 eV. The distribution of nitrogen in the PVC substrate and ANF membrane was investigated by x-ray energy dispersive spectroscopy（EDS, GENES1S60S, USA）. SEM images were obtained on a field emission scanning electron microscopy (FESEM, Hitachi S-4800, Japan). Membrane surface charge was determined by the streaming potential method using a SurPASS electrokinetic analyzer (Anton Paar GmbH, Austria) with an electrolyte solution of 0.001 M potassium chloride (KCl), whereas 0.5 M hydrogen chloride (HCl) solution and 0.05 M potassium hydroxide (KOH) solution were used to adjusted pH values of the electrolyte solution. The streaming potential results were then calculated by its built-in software using Helmholtz-Smoluchowski equation to determine the membrane zeta potential. To

investigate the charge properties of interlayer between substrate and outermost surface of the ANF membranes, flat sheet ANF membranes were prepared using homemade flat PVC membrane as substrate. The as-prepared ANF membrane was placed on a steel mesh (mesh number: 400) with the PVC substrate facing up. The PVC substrate was peeled off with the method described in the literature [32]. The sample on the steel mesh was used to investigate the charge properties of the interlayer. DBES conducted using PAS coupled with a variable mono-energy slow positron beam, was used to characterize the membrane micro-structure as a function of positron incident energy. The detail information regarding the use of PAS can be found in our previous publications [33-34].

2.4. Membrane performance test

Separation performance was assessed in a lab-made cross-flow filtration system at 25 ℃. All performance data were collected after steady-state flow conditions had been reached. The pure water permeability（PWP，$L \cdot m^{-2} \cdot h^{-1} \cdot bar^{-1}$) of all membranes were tested before solutes rejection experiments and calculated using the following equation:

$$PWP = \frac{Q}{A \triangle P} \quad (1)$$

Where Q is the volumetric permeation flow rate ($L \cdot h^{-1}$), A is the valid membrane filtration area (m^2), and ΔP is the trans-membrane pressure (bar).

Afterwards, single salt and neutral organic solute rejection experiments were

conducted on aqueous $MgCl_2$ (1000 mg/L), $MgSO_4$ (1000 mg/L), Na_2SO_4 (1000 mg/L), NaCl (500 mg/L), $CaCl_2$ (1000 mg/L), $Pb(NO_3)_2$ (500 mg/L), glucose (200 mg/L) and sucrose (200 mg/L) in the cross-flow filtration system at an operation pressure of 3.5 bar. Solute rejection, *R* (%), was determined from the solute concentration in the feed (C_f) and permeate (C_p) based on the following equation. Concentration of electrolyte and neutral organic solute were measured with a conductivity meter (DDS-11A) and TOC analyzer (TOC-VCSH, Shimadzu, Japan), respectively.

$$R = \left(1 - \frac{C_p}{C_f}\right) \times 100\% \quad (2)$$

All experiments were repeated three times for three replicate samples and averaged.

2.5. TMC treatment and K^+ rejection experiments

TMC treatments: To ascertain the role of the interlayer between PVC substrate and outermost surface of ANF membranes during separation process, the TMC treatment experiment was designed and was carried out as follows: A 0.1 % TMC/hexane solution was introduced into the shell side of the ANF membrane modules for 10 min. Prior to the treatment, the wet NF membrane modules were immersed into ethanol for 30 min to substitute water trapped in pores and then dried at ambient temperature for 60 min before TMC treatments to guarantee that TMC/hexane solution was able to contact the interlayer during TMC treatments. For comparison purpose, the same treatment was also applied on NF-PES and NF-PVC membranes.

K^+ rejection experiments

To further explore the transport and separation mechanism of the ANF membrane, effect of feed pH on K^+ rejection was investigated. A 200 mg/L KCl solution was used as original feed and 0.5 M HCl solution and 0.5 M KOH solution were used to adjust pH values of the feed solution. K^+ concentration in the feed and permeate solutions was determined by an inductively coupled plasma optical emission spectrometry (ICP-OES, Optima 8000, Perkin Elmer, USA).

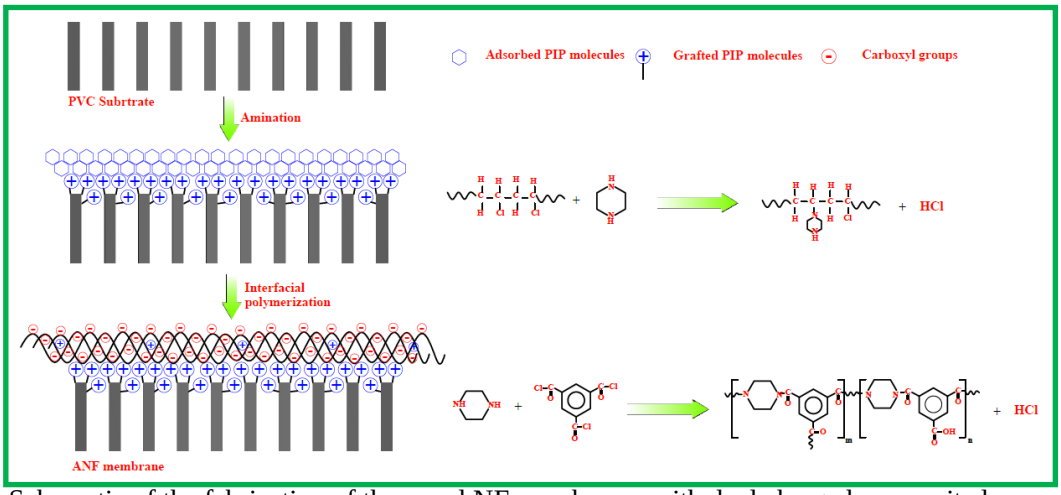

Fig. 1. Schematic of the fabrication of the novel NF membranes with dual charged composite layers via amination-interfacial polymerization. Proposed mechanisms of amination and interfacial polymerization are present.

3. Results and discussions

3.1. Characterization of membranes

The surface morphologies of PVC, ANF and NF-PVC membranes are shown in Fig. 2. Compared with the porous surface of PVC substrate, both the ANF and NF-PVC

membrane exhibited a dense composite layer and typical nodular structure resulted from the polymerization of PIP and TMC [25]. There is no obvious difference of surface morphology of the two kinds of NF membranes and thus other characterizations were performed thereafter.

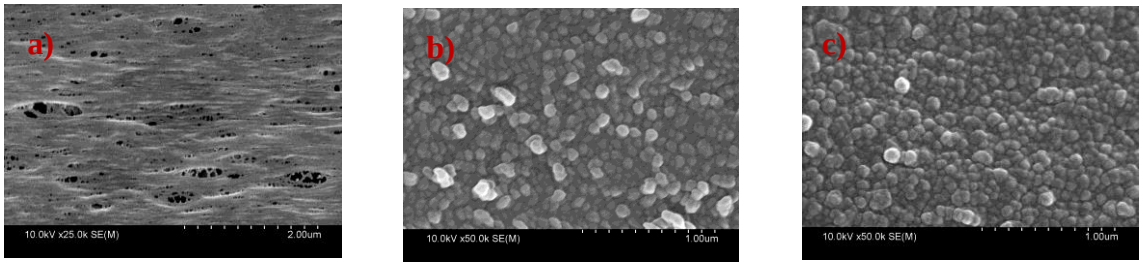

Fig. 2. Surface SEM morphology of a) PVC, b) ANF and c) NF-PVC membrane.

Fig. 3 shows the FT-IR spectra of PVC, APVC, ANF membranes. Absorptions can be found at around 1660 cm^{-1} (C=O stretching) in the spectrums of the three membranes, because vinisol was used as additive during PVC substrate membrane preparation. Compared with the spectrum of PVC membranes, the spectrum of APVC and ANF membranes exhibit the absorption peaks around 1050 cm^{-1}, which stand for the tertiary C-N groups result from the nucleophilic substitution between PVC and PIP [35].

Furthermore, XPS spectra of PVC substrate and APVC membrane are presented in Fig. 4 and the XPS data of element contents on the membrane surface are given in Table 1. Compared with PVC substrate, a new peak (N1s) appeared in the spectrum of APVC membrane, which indicates that PIP was successfully grafted into PVC substrate. Table

1 shows that the atom percentage of chlorine declined from 20.37 % of PVC substrate to 15.92 % of APVC membrane and the atom percentage of nitrogen was 4.05 % on surface of APVC membrane, which should be attributed to the nucleophilic substitution reaction between PVC and PIP. A proposed mechanism of the substitution reaction was drawn in Fig. 1 [36-37].

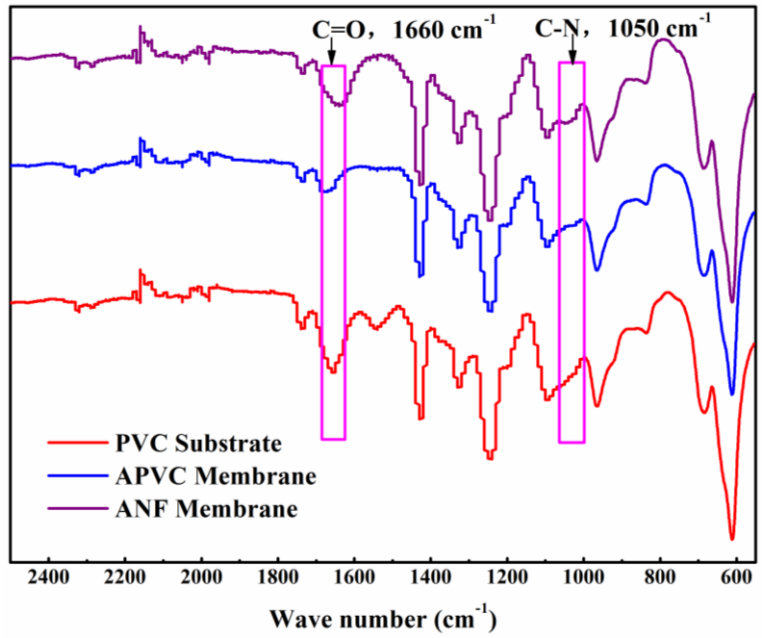

Fig. 3. Comparison of FT-IR spectra among the PVC substrate, APVC membrane and ANF membrane.

It is worthy to note that both the surface of ANF1.0 and NF-PVC membranes appeared chlorine and their atom percentage is 2.98 % and 1.60 %, respectively. Since the detection depth of XPS measurement in this study is affected by the thickness and density of the composite layer, the higher chlorine content of the ANF1.0 membrane probably be attributed to its thinner or looser composite layer.

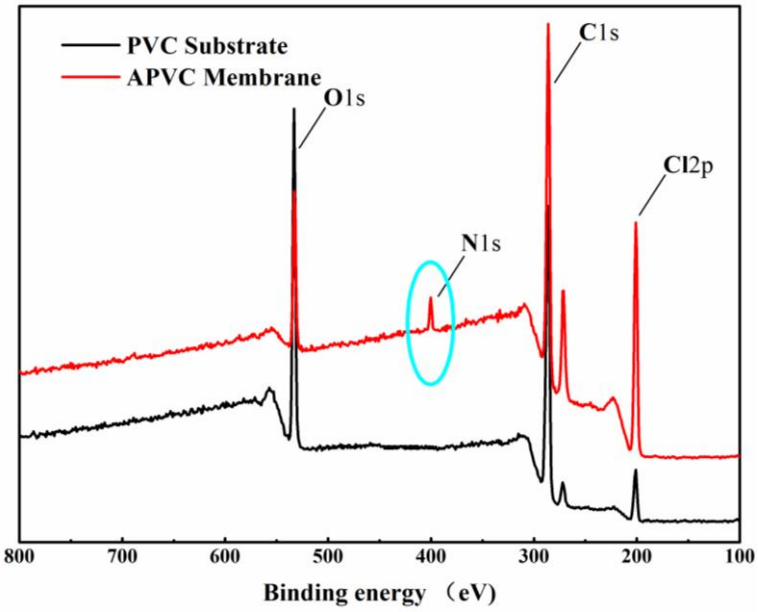

Fig. 4. Wide scan XPS spectra of PVC substrate and APVC membrane.

Table 1. Surface elemental composition of PVC, APVC, ANF1.0 and NF-PVC membranes

Membrane	Surface elemental composition (At. %)			
	C1s	O1s	N1s	Cl2p
PVC	68.04	11.58	0.00	20.38
APVC	66.59	13.44	4.05	15.92
NF-PVC	71.01	18.68	8.71	1.60
ANF1.0	72.85	13.51	10.66	2.98

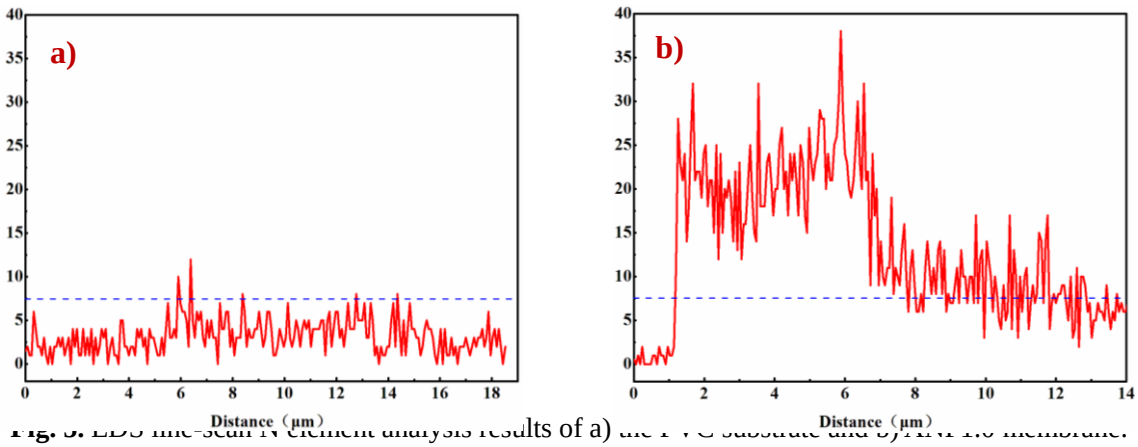

Fig. 5. EDS line-scan N element analysis results of a) the PVC substrate and b) ANF1.0 membrane.

The distribution of Nitrogen in the PVC substrate and ANF membrane was

investigated by EDS line-scan nitrogen element analysis. The analytical results (Fig. 5) show that nitrogen content of composite layer is apparently higher than that of the PVC substrate, and the PIP not only existed in IP formed layer, but also was grafted on substrate away from the active layer.

Table 2. Zeta potential of outermost and back surface of membranes at pH=6.5

Membrane	Outermost surface (mV)	Back surface (mV)
PVC	-31.30	----
APVC	-3.80	----
ANF1.0	-6.67	36.52
NF-PVC	-29.65	-50.76

The APVC membrane was fabricated under a PIP concentration of 1.0 % （w/v）.

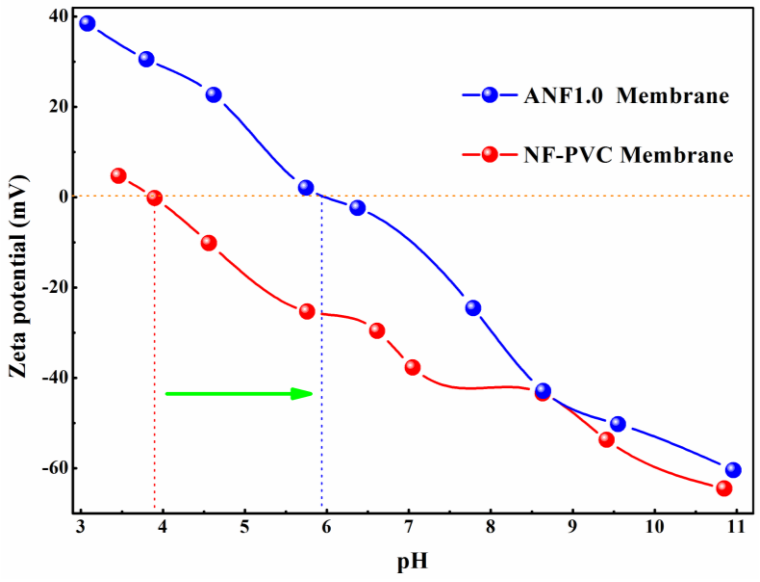

Fig. 6. Zeta potential of NF-PVC and ANF1.0 membrane at pH ranging from 3 to 11.

As vinisol was used as additive during PVC substrate preparation, the pure PVC membrane gives a zeta potential of -31.3 mV at pH=6.5. The obviously increase of zeta potential from -31.3 mV to -3.8 mV should be attributed to the protonation of amine

group brought from PIP molecules grafted on PVC substrate. The zeta potential results of the NF-PVC and ANF1.0 membrane are presented in Fig. 6. Due to the hydrolysis of residual acyl chloride after IP process, both NF-PVC and ANF1.0 membranes exhibits negative charges at pH=6.5. However, it is worth to note that the isoelectric point of ANF1.0 membrane comes to around pH=6 and that of NF-PVC membrane is around pH=4. To investigate the charge properties of the interlayer between outermost surface and PVC substrate, zeta potential at pH=6.5 of back surface of the composite layer was analyzed after etching off the PVC support membrane. As shown in Table 2, zeta potential of outermost surface and back surface of ANF1.0 membrane is -6.67 and 36.52 mV, respectively, confirming the dual charged composite layer structure directly. However, both top and back surfaces of NF-PVC membrane are negatively charged. The obvious shifting of isoelectric point from pH=4 to pH=6 and the magically conversion from negatively charged APVC membrane to positively charged interlayer could be explained as following. As specified previously, there are two kinds of PIP molecules: the adsorbed ones and the grafted ones after amination of PVC membranes, the more positively charged ANF1.0 membrane including outermost surface and interlayer than the typical NF-PVC membrane indicate that the composite layer of ANF1.0 membrane contain more amine groups than that of NF-PVC membrane which was evidenced by the XPS results in Table 1. Also, since tertiary amine group is more

easily to be protonated than secondary amine group, back surface of composite layer of ANF membrane become positively charged even though the APVC membrane still exhibit weak negative charge.

To improve our understanding of the microstructure of ANF membranes, composite layers of NF membranes were characterized by PAS. S parameters obtained as a function of the positron incident energy or depth for the NF-PVC and ANF1.0 membranes is shown in Fig. 7. The two NF membranes show a similar variation tendency of S parameters with depth, exhibiting a sharp increase before a platform and then gradually increasing to the peaks. The initial sharp increase could be attributed to the back diffusion and scattering of positroniums near the membrane surface and the platform should be corresponded to the polyamide layer, while the gradual increases to peak should be due to the transition from composite layer to substrate [33, 38].

The thicknesses of the composite layer obtained from curves in Fig. 7 indicates that ANF1.0 membrane (69 nm) exhibits a thinner composite layer when compared to the NF-PVC membrane (124 nm). Moreover, the ANF1.0 membrane has a larger S parameter which indicates that the ANF1.0 membrane has a looser microstructure. These results are in accordance with the supposition based on XPS results in Table 1. Both the results of thickness measurement and free volume indicate that the ANF membranes have weaker size exclusion than that of IP made NF membrane during

filtration processes.

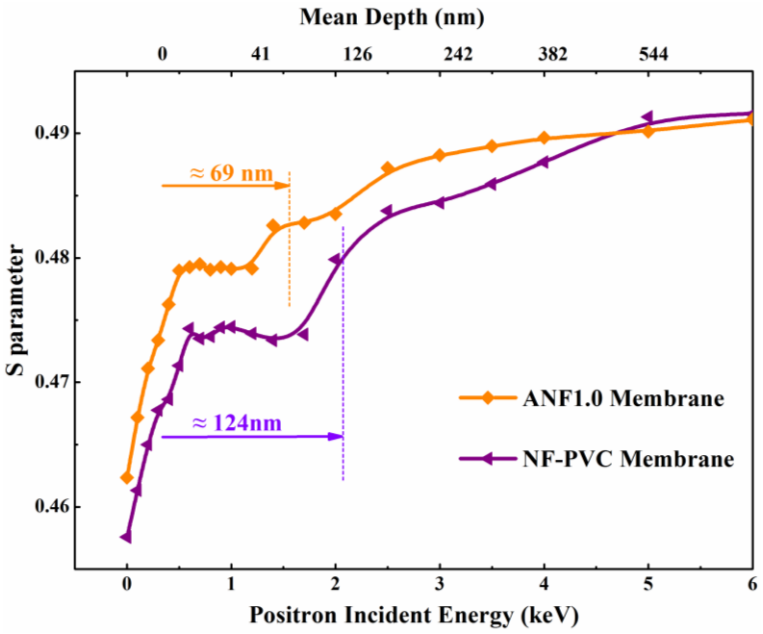

Fig. 7. S parameter as a function of positron incident energy and VEPFIT fitting for NF-PVC and ANF1.0 membranes

3.2 Separation performance of the ANF membranes

The separation performance of the ANF membranes is determined by their ability to reject a series of neutral solutes and single inorganic salts. Neutral solutes rejection tests were always conducted to estimate the density of composite layer [39]. The molecular weight of glucose and sucrose and their rejection by NF membranes are listed in Table 3. Both the ANF1.0 and NF-PVC membranes exhibit a similar rejection to sucrose（about 98 %）due to its large molecular weight. However, ANF1.0 membranes exhibit a relatively lower rejection towards glucose comparing to NF-PVC membrane due to its relatively loose microstructure as confirmed by the PAS analysis.

Table 3. Rejection of composite membranes to various neutral solutes

Solute	Molecular Weight (Da)	Solute Rejection (%)	
		ANF1.0	NF-PVC
Glucose	180	90.3	91.7
Sucrose	342	98.1	98.2

Tested at 0.35MPa using 200 mg/L neutral solute solutions.

Fig. 8 shows the PWP and salts rejection ($MgCl_2$, Na_2SO_4) when the concentration of PIP aqueous solution increased from 0.1 to 2.0% (w/v) with constant TMC concentration (0.1% w/v). The variation tendency of PWP corresponding to the increasing of PIP concentration is dramatically different from the conventional IP made NF membranes. The PWP of ANF membranes increased when increased PIP concentration from 0.1 % to 0.5 %, which could probably be attributed to the increasing hydrophilicity of amine-enriched layer. When further increasing the PIP concentration to 2.0 %, the PWP decreased gradually. The interpretation from this phenomenon is probably that thickness of composite layer increased and structure of composite layer become denser [40]. The variation tendency of salts rejection corresponding to the increasing of PIP concentration is similar to related reports [41-42]. Nevertheless, the salt rejection of the all ANF membranes corresponding to different types of feed solutions is $MgCl_2 \approx MgSO_4 > Na_2SO_4 > NaCl$, which is similar to a positively charged NF membrane. However, the separation performance of NF-PES and NF-PVC membranes exhibit a salts rejection order of $Na_2SO_4 \approx MgSO_4 > MgCl_2 > NaCl$ in accordance with the separation performance of typical negatively charged NF

membrane [43-44].

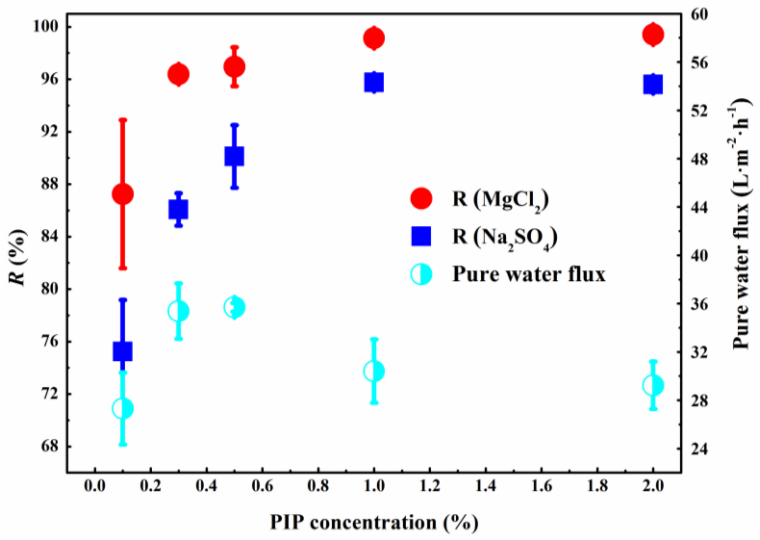

Fig. 8. PWP and salts (Na_2SO_4, $MgCl_2$) rejection of ANF membranes as a function of PIP concentration.

Separation experiments data (Fig. 9) indicate that the ANF1.0 membranes exhibit super-high rejection towards both multivalent anions and multivalent metal cations. Moreover, desirable results would be obtained when compared the performance of ANF1.0 membranes to commercial NF membranes with composite layer making from IP of PIP and TMC. In particular, compared with the DOW® NF270, the ANF1.0 membrane exhibited a remarkable ≈ 60 % enhancement in rejection toward $Pb(NO_3)_2$, $CaCl_2$, and $MgCl_2$ and comparable retention to Na_2SO_4. Significantly, the ANF1.0 membranes exhibited a reasonably high PWP of 8.7 $L \cdot m^{-2} \cdot h^{-1} \cdot bar^{-1}$. The promising preliminary results indicate that the ANF membranes will have high potential in numerous applications, such as potable water treatment, pretreatment of RO seawater

desalination.

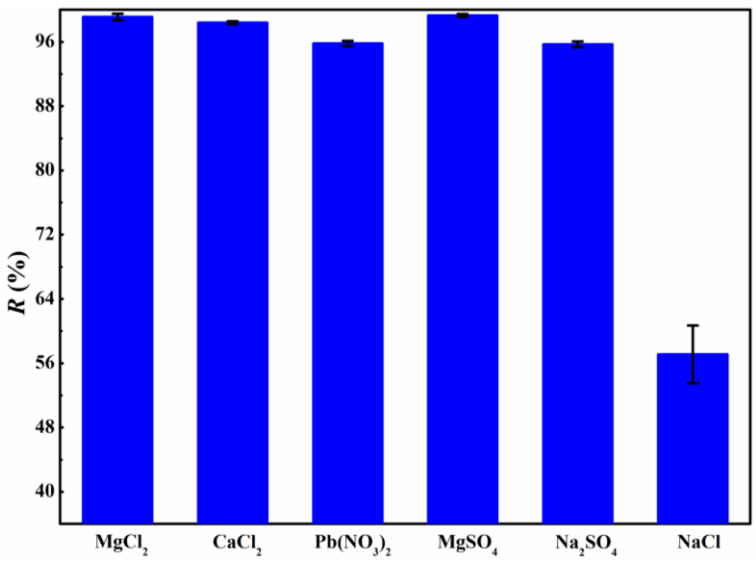

Fig. 9. Rejection of ANF1.0 to different salts. All performance tests were conducted at an operating pressure of 3.5 bar using 1000 mg/L salt solution except for $Pb(NO_3)_2$ and NaCl (500 mg/L).

As aforementioned, the main rejection mechanism of NF membranes are size exclusion and electrostatic interaction. Results of PAS test and neutral solutes reject experiments reveal that the ANF membranes exhibit a relative loose microstructure suggesting the electrostatic interaction play a major role in this case. Therefore, it can be concluded that the significant upgraded separation performance of ANF membranes could attribute to the *co*-separation of the dual charged layer.

3.3 Transport and separation mechanism

TMC treatment experiments were employed to ascertain the role of the interlayer between PVC substrate and outermost surface of ANF membranes during desalination

process. As shown in fig. 10, the rejection for $MgCl_2$ of NF-PES and NF-PVC membrane after TMC treated increases from 79.0 % to 82.0 % and 77.0 % to 80.0 %, respectively. This phenomena is more likely attributed to the reaction between TMC and residual amine groups in composite layer resulting in a tighter thin film. As a consequence, salts rejection of these two TMC treated membranes increase and flux decrease. The evaluation of Na_2SO_4 rejection of the NF-PES and NF-PVC membrane after TMC treated no only be attributed to the tighter thin film but the more negatively charged result from the hydrolysis of residual acyl chloride. Interestingly, the rejections of TMC treated ANF1.0 to $MgCl_2$ decreases from 99.0 % to 93.0 % and to Na_2SO_4 rejection increases from 96.0 % to 98.0 %. However, rejection order of NF-PES and NF-PVC membranes did not change after TMC treatment. Previous studies have demonstrated that the dramatic change of rejection order always attributes to the reversal of membrane charge property [45-46]. The separation performance change after TMC treated can be explained as follows. The amine enriched positively charged interlayer become carboxyl terminated negatively charged after sufficient reaction with TMC and hydrolysis of acyl chloride groups. Moreover, the sufficient reaction of TMC and amine groups in the interlayer increases the hydraulic resistance which lead to the dramatic decrease of PWP from 8.7 to 3.8 $L \cdot m^{-2} \cdot h^{-1} \cdot bar^{-1}$ [47]. These results not only further demonstrate the existence of the positively charged interlayer but also reveal its

role in the desalination process.

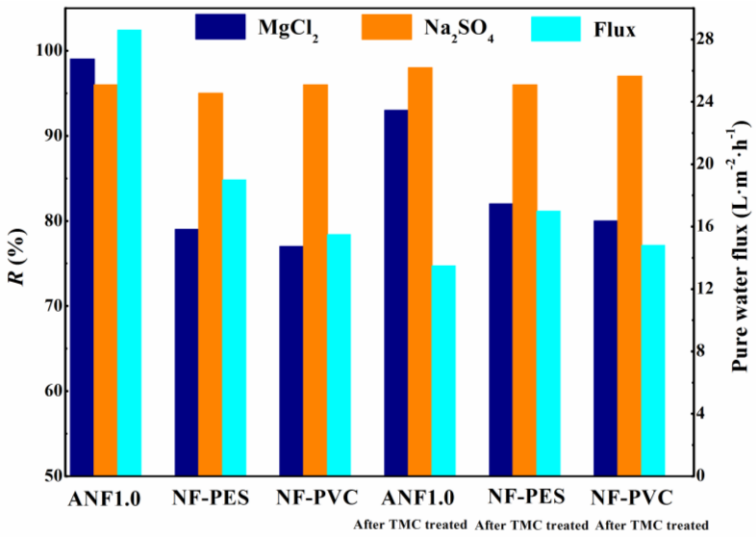

Fig. 10. Separation performance of NF and TMC treated NF membranes

Furthermore, effect of pH on K^+ rejection was explored. Base on the fact that the electrostatic interaction between the charged membrane surface and ions performed a minimum at around isoelectric point of membrane surface, minimum salts rejection should obtain at the pH equal to isoelectric point [48]. However, as shown in Fig. 11, the lowest K^+ rejection obtained was shifted to pH around 7 apart from isoelectric point of the outermost surface at pH around 6 attributing to the synergistic effect of the dually charged layer. Proposed charge transformation with pH of the dually charged composite layer was depicted in Fig. 12 to minutely explain the phenomenon in Fig. 11. Charge of dual composite layer of ANF1.0 membrane both decreased with increasing feed pH from pH 3 to pH 6, as a consequence, K^+ rejection of ANF1.0 membrane decreased

from pH 3 to pH 6 gradually. Even though the negative outermost surface charge increased when further increasing feed pH to pH 7, K^+ rejection of the ANF1.0 membrane keep decreasing. This could be attributed to the decrease of positive interlayer charge. The positive interlayer charge would keep decreasing and become negatively charged with further increasing feed pH from pH 7. It is worth to note that the minimum salts rejection obtained at pH 7 do not represent the isoelectric point of the interlayer, but the weakest point of synergistic effect of the dually charged composite layer.

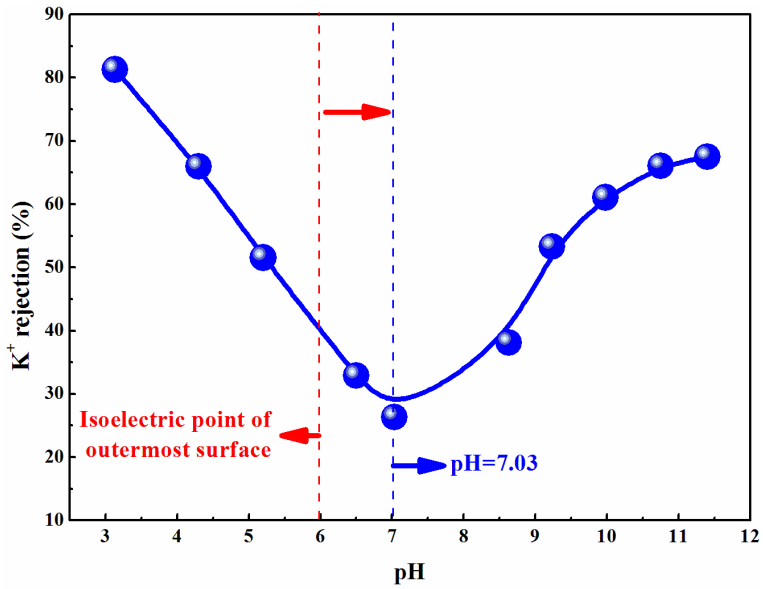

Fig. 11. Effect of feed pH on K^+ rejection of ANF1.0 membrane.

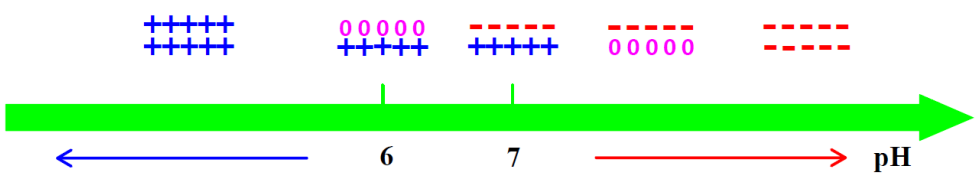

Fig. 12. Proposed charge transformation with pH of the dual charged composite layer.

A schematic comparison of the proposed structure of composite layers fabricated via A-IP and IP and their transport and separation mechanism are shown in Fig. 13. Multivalent anions (e.g., $Cr_2O_7^{2-}$, SO_4^{2-}) are mainly rejected by the negatively charged outermost surface due to the electrostatic repulsion. However, if the multivalent anions had passed through the outermost layer, they would easily enter the permeation due to the strong affinity between anions and -NH- groups in the interlayer. Although the multivalent cations have affinity to the outermost surface, part of cations still will be rejected by size exclusion of the outermost surface. Since the small size cations, which have entered the pore channel of the outmost surface, will be hindered by the positively charged amine enriched interlayer and trapped in the channel close to the interlayer. Therefore, the pore channel of the outermost surface close to the interlayer will be also positively charged, which will further improve the cation rejection.

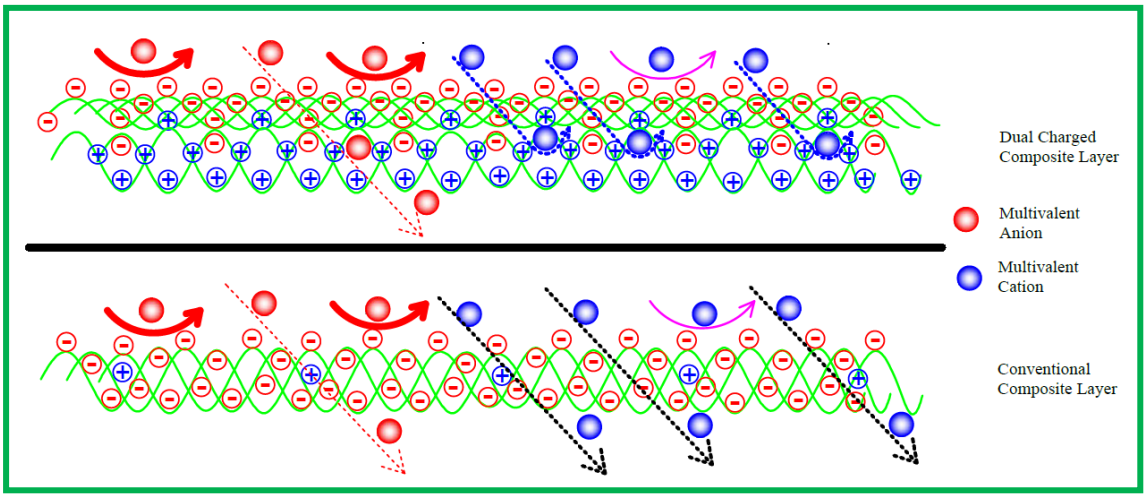

Fig. 13. Schematic illustration showing the proposed structure of composite layers fabricated via A-IP and conventional IP, respectively.

3.4 Stability of NF membranes in long-term operation

The ANF1.0 and NF-PVC membrane were operated with continuous filtration to evaluate the long-term operation stability of the dually charged composite layer. Flux of these two NF membrane varied little during the filtration. As shown in Fig. 14, salt rejection of ANF1.0 membrane varied little with operation time and the rejection remaining over 98.0% which demonstrates that there are no unfavorable interactions between positively charged layer and negatively charged layer and the ANF1.0 membrane possess good durability in long-term operation process. For comparison, salt rejection of NF-PVC membrane exhibited a sharp decrease in first five hours which could be attributed to relatively weak interfacial adhesion.

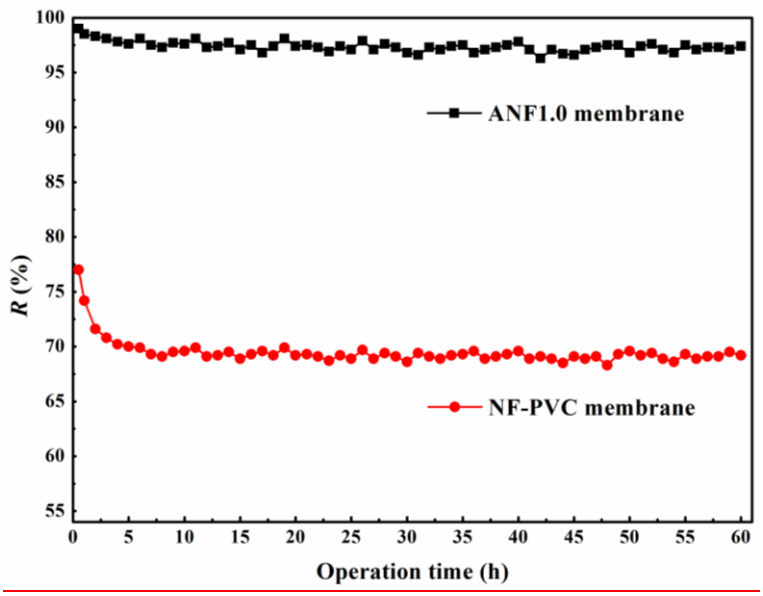

Fig. 14. Long-term stability of the ANF1.0 and NF-PVC membrane. Tested at 0.35 MPa, room temperature with 1000 mg/L $MgCl_2$ aqueous solution.

4. Conclusions

In summary, this paper reported a composite membrane consists of a positively charged interlayer sandwiched between substrate and negatively charged outermost surface for the first time. A facile method for preparing the dually charged composite layer NF membranes via A-IP on PVC substrate is presented. The re-structured membrane exhibit super-high multivalent salts rejection and a reasonably high flux. The significant upgraded separation performance of ANF membranes can be attributed to the synergistic effect of the dually charged layer. The promising preliminary results in this study provide a useful platform to promote the separation performance of NF membrane. The ANF membrane with super-high multivalent-salt rejection is also promising in

application in drinking water treatment and pretreatment of RO seawater desalination.

Acknowledgments

This study was supported by National Natural Science Foundation of China (51278336, 51578376, 21576210, 21306135), Research Program of Application Foundation and Advanced Technology, Tianjin, China (15JCZDJC37500, 13JCQNJC08800), Program for Changjiang Scholars and Innovative Research Team in University (PCSIRI) of Ministry of Education of China (Grand no. IRI13084).

References

(1) M. Elimelech, W. A. Phillip, The future of seawater desalination: energy, technology, and the environment, Science 333 (2011**)** 712-717.

(2) Q. Schiermeier, Water risk as world warms first comprehensive global-impact project shows that water scarcity is a major worry, Nature 505 (2014) 10-11.

(3) M. A. Shannon, P. W. Bohn, M. Elimelech, J. G. Georgiadis, B. J. Marinas, A. M. Mayes, Science and technology for water purification in the coming decades, Nature 452 (2008) 301-310.

(4) S. J. Tesh, T. B. Scott, Nano-composites for water remediation: a review, Adv. Mater. 26 (2014) 6056-6068.

(5) A. G. Fane, R. Wang, M. X. Hu, Synthetic membranes for water purification: status and future, Angew. Chem. Int. Ed. 54 (2015) 3368-3386.

(6) S. Qu, T. Dilenschneider, W. A. Phillip, Preparation of chemically-tailored copolymer membranes with tunable ion transport properties, ACS Appl. Mater. Interfaces 7 (2015) 19746-19754.

(7) F. Fu, Q. Wang, Removal of heavy metal ions from wastewaters: a review, J. Environ. Manage. 92 (2011) 407-418.

(8) B. A. M. Al-Rashdi, D. J. Johnson, N. Hilal, Removal of heavy metal ions by nanofiltration, Desalination 315 (2013) 2-17.

(9) J. Schaep, B. Van der Bruggen, S. Uytterhoeven, R. Croux, C. Vandecasteele, D. Wilms, E. Van Houtte, F. Vanlerberghe, Removal of hardness from groundwater by nanofiltration, Desalination 119 (1998) 295-302.

(10) W. Fang, L. Shi, R. Wang, Interfacially polymerized composite nanofiltration hollow fiber membranes for low-pressure water softening, J. Membr. Sci. 430 (2013) 129-139.

(11) Y. Gao, A. M. S. D. Jubera, B. J. Marinas, J. S. Moore, Nanofiltration membranes with modified active layer using aromatic polyamide dendrimers, Adv. Funct. Mater. 23 (2013) 598-607.

(12) A.W. Mohammad, Y. H. Teow, W. L. Ang, Y. T. Chung, D. L. Oatley-Radcliffe, N. Hilal, Nanofiltration membranes review: recent advances and future prospects, Desalination 356 (2015) 226-254.

(13) C. Wu, S. Zhang, D. Yang, X. Jian, Preparation, characterization and application of a novel thermal stable composite nanofiltration membrane, J. Membr. Sci. 326 (2009) 429-434.

(14) A. K. Ghosha, E. M. V. Hoek, Impacts of support membrane structure and chemistry on polyamide-polysulfone interfacial composite membranes, J. Membr. Sci. 336 (2009) 140-148.

(15) F. G. Donnan, Theory of membrane equilibria and membrane potentials in the presence of non-dialysing electrolytes. A contribution to physical-chemical physiology, J. Membr. Sci. 100 (1995) 45-55.

(16) K. L. Cho, A. J. Hill, F. Caruso, S. E. Kentish, Chlorine resistant glutaraldehyde crosslinked polyelectrolyte multilayer membranes for desalination, Adv. Mater. 27 (2015) 2791-2796.

(17) C. Liu, L. Shi, R. Wang, Crosslinked layer-by-layer polyelectrolyte nanofiltration hollow fiber membrane for low-pressure water softening with the presence of SO_4^{2-} in feed Water, J. Membr. Sci. 486 (2015) 169-176.

(18) Z. Thong, G. Han, Y. Cui, J. Gao, T. S. Chung, S. Y. Chan, S. Wei, Novel nanofiltration membranes consisting of a sulfonated pentablock copolymer rejection layer for heavy metal removal, Environ. Sci. Technol. 48 (2014) 13880−13887.

(19) J. Gao, S. P. Sun, W. P. Zhu, T. S. Chung, Chelating polymer modified P84

nanofiltration hollow fiber membranes for high efficient heavy metal removal, Water Res. 63 (2014) 252-261.

(20) J. Garcia-Aleman, J. M. Dickson, Permeation of mixed-salt solutions with commercial and pore-filled nanofiltration membranes: membrane charge inversion phenomena, J. Membr. Sci. 239 (2004) 163–172.

(21) S. Lee, C. H. Lee, Effect of membrane properties and pretreatment on flux and NOM rejection in surface water nanofiltration, Sep. Purif. Technol. 56 (2007) 1-8.

(22) D. Wu, S. Yu, D. Lawless, X. Feng, Thin film composite nanofiltration membranes fabricated from polymeric amine polyethylenimine imbedded with monomeric amine piperazine for enhanced salt separations, React. Funct. Polym. 86 (2015) 168-183.

(23) C. Ba, J. Economy, Preparation and characterization of a neutrally charged antifouling nanofiltration membrane by coating a layer of sulfonated poly (ether ether ketone) on a positively charged nanofiltration membrane, J. Membr. Sci. 362 (2010) 192-201.

(24) S. Cheng, D. L. Oatley, P. M. Williams, C. J. Wright, Characterisation and application of a novel positively charged nanofiltration membrane for the treatment of textile industry wastewaters, Water Res. 46 (2012) 33-42.

(25) F. Yang, S. Zhang, D. Yang, X. Jian, Preparation and characterization of polypiperazine amide/PPESK hollow fiber composite nanofiltration membrane, J.

Membr. Sci. 301 (2007) 85-92.

(26) J. Tian, Z. Chen, Y. Yang, H. Liang, J. Nan, G. Li, Consecutive chemical cleaning of fouled PVC membrane using NaOH and ethanol during ultrafiltration of river water, Water Res. 44 (2010) 59-68.

(27) X. Zhang, Y. Chen, A. H. Konsowa, X. Zhu, J. C. Crittenden, Evaluation of an innovative polyvinyl chloride (PVC) ultrafiltration membrane for wastewater treatment, Sep. Purif. Technol. 70 (2009) 71-78.

(28) S. Moulay, Chemical modification of poly (vinyl chloride)-still on the run, Prog. Polym. Sci. 35 (2010) 303-331.

(29) B. Balakrishnan, D. S. Kumar, Y. Yoshida, A. Jayakrishnan, Chemical modification of poly(vinyl chloride) resin using poly(ethylene glycol) to improve blood compatibility, Biomaterials 26 (2005) 3495-3502.

(30) I. S. Ahamed, A. K. Ghonaim, A. A. Abdel Hakim, M. M. Moustafa, A. H. Kamal El-Din, Synthesis and characterization of some polymers for removing of some heavy metal ions of industrial wastewater, J. Appl. Sci. Res. 4 (2008) 1946-1958.

(31) J. T. S. Allan, L. E. Prest, E. B. Easton, The sulfonation of polyvinyl chloride: synthesis and characterization for proton conducting membrane applications, J. Membr. Sci. 489 (2015) 175-182.

(32) H. Yan, X. Miao, J. Xu, G. Pan, Y. Zhang, Y. Shi, M. Guo, Y. Liu, The porous

structure of the fully-aromatic polyamide film in reverse osmosis membranes, J. Membr. Sci. 475 (2015) 504-510.

(33) K. L. Tung, Y. C. Jean, D. Nanda, K. R. Lee, W. S. Hung, C. H. Lo, J. Y. Lai, Characterization of multilayer nanofiltration membranes using positron annihilation spectroscopy, J. Membr. Sci. 343 (2009) 147-156.

(34) H. Chen, W. S. Hung, J. H. Lo, S. H. Huang, M. L. Cheng, G. Liu, K. R. Lee, J. Y. Lai, Y. M. Sun, C. C. Hu, R. Suzuki, T. Ohdaira, N. Oshima, Y. C. Jean, Free-volume depth profile of polymeric membranes studied by positron annihilation spectroscopy: layer structure from interfacial polymerization, Macromolecules 40 (2007) 7542-7557.

(35) Y. Zheng, G. Yao, Q. Cheng, S. Yu, M. Liu, C. Gao, Positively charged thin-film composite hollow fiber nanofiltration membrane for the removal of cationic dyes through submerged filtration, Desalination 328 (2013) 42-50.

(36) R. P. Kusy, J. Q. Whitley, R. P. Buck, V. V. Cosofret, E. Lindner, Development of piperazine grafted poly(vinyl chloride)s for fixed site proton carriers, J. Mater. Sci. Lett. 13 (1994) 849-851.

(37) J. Q. Whitley, R. P. Kusy, Syntheses of aminated poly(vinyl chloride)s using methyl piperazine for the development of pH-selective membranes, Polymer 39 (1998) 441-447.

(38) Y. Cui, X. Y. Liu, T. S. Chung, Enhanced osmotic energy generation from salinity gradients by modifying thin film composite membranes, Chem. Eng. J. 242 (2014) 195-

203.

(39) Y. Li, Y. Su, X. Zhao, X. He, R. Zhang, J. Zhao, X. Fan, Z. Jiang, Antifouling, high-flux nanofiltration membranes enabled by dual functional polydopamine, ACS Appl. Mater. Interfaces 6 (2014) 5548-5557.

(40) L. Li, S. B. Zhang, X. S. Zhang, Preparation and characterization of poly(piperazineamide) composite nanofiltration membrane by interfacial polymerization of 3,3′,5,5′-biphenyl tetraacyl chloride and piperazine, J. Membr. Sci. 335 (2009) 133-139.

(41) Y. Li, Y. Su, J. Li, X. Zhao, R. Zhang, X. Fan, J. Zhu, Y. Ma, Y. Liu, Z. Jiang, Preparation of thin film composite nanofiltration membrane with improved structural stability through the mediation of polydopamine, J. Membr. Sci. 476 (2015) 10-19.

(42) D. Hu, Z. L. Xu, C. Chen, Polypiperazine-amide nanofiltration membrane containing silica nanoparticles prepared by interfacial polymerization, Desalination 301 (2012) 75-81.

(43) X. Wei, X. Kong, C. Sun, J. Chen, Characterization and application of a thin-film composite nanofiltration hollow fiber membrane for dye desalination and concentration, Chem. Eng. J. 223 (2013) 172-182.

(44) Y. Han, Y. Jiang, C. Gao, High-flux graphene oxide nanofiltration membrane intercalated by carbon nanotubes, ACS Appl. Mater. Interfaces 7 (2015) 8147-8155.

(45) H. Qian, S. Li, J. Zheng, S. Zhang, Ultrathin films of organic networks as nanofiltration membranes via solution-based molecular layer deposition, Langmuir 28 (2012) 17803-17810.

(46) J. Grooth, D. M. Reurink, J. Ploegmakers, W. M. Vos, K. Nijmeijer, Charged micropollutant removal with hollow fiber nanofiltration membranes based on polycation/polyzwitterion/polyanion multilayers, ACS Appl. Mater. Interfaces 6 (2014) 17009-17017.

(47) J. E. Gu, S. Lee, C. M. Stafford, J. S. Lee, W. Choi, B. Y. Kim, K. Y. Baek, E. P. Chan, J. Y. Chung, J. Bang, J. H. Lee, Molecular layer-by-layer assembled thin-film composite membranes for water desalination, Adv. Mater. 25 (2013) 4778-4782.

(48) J. J. Qin, M. H. Oo, H. Lee, B. Coniglio, Effect of feed pH on permeate pH and ion rejection under acidic conditions in NF process, J. Membr. Sci. 232 (2004) 153-159.